Chin.J.Geochem.(2014)33:365–373
DOI: 10.1007/s11631-014-0699-6

Analysis of platinum-group elements in drill core samples from the Meishan Permian-Triassic boundary section, China

XU Lin[1*] and LIN Yangting[2]

[1] *Key Laboratory of Lunar and Deep Space Exploration, National Astronomical Observatories, Chinese Academy of Sciences, Beijing 100012, China*

[2] *State Key Laboratory of Lithospheric Evolution, Institute of Geology and Geophysics, Chinese Academy of Sciences, Beijing 100029, China*

[*] *Corresponding author, E-mail: xul@nao.cas.cn*

Received September 1, 2013, accepted March 20, 2014

Abstract There is a long-standing controversy of what triggered the extinction at the Permian-Triassic boundary, the most severe mass extinction in the geologic record, including flood basaltic volcanism and/or bolide impact hypothesis. In order to clarify various pieces of evidence for the mass extinction event at the Permian-Triassic boundary, some researchers from some laboratories throughout the world have made a comprehensive study on a group of samples from the Meishan area of China. Some fresh core samples from the Permian-Triassic boundary in the Meishan area were analyzed in this study. The results showed that there is no Ir anomaly. Moreover, the PGEs patterns of those samples show obvious differentiation characteristics, that is different from the case encountered in meteorites. So no evidence supports the hypothesis of extraterrestrial impact. In contrast, the PGEs patterns are similar to those of Siberian and Emeishan basalts, which indicates that those PGEs are derived mainly from the basalts, lending a support to the correlation between mass extinction at the Permian-Triassic boundary and flood basaltic volcanism. This study has also confirmed the results for samples from section C prior to the analysis of the samples.

Key words Permian-Triassic boundary event; platinum-group element; mass extinction; extraterrestrial impact; basaltic volcanic eruption

1 Introduction

The most severe living things extinction event on the Earth took place 252.28±0.08 million years ago between the Permian and Triassic boundary geologic periods, as well as between the Paleozoic and the Mesozoic, with up to 90% of all marine species and 70% of terrestrial vertebrate species having being extincted (Erwin, 1994; Jin et al., 2000; Benton et al., 2004). The extinction characteristics of P-T boundary and the sedimentary records show that a series of sudden major geological events may have occurred at that time. Along with the biological extinction event, the ecosystems experienced dramatic changes, such as marine anoxia (Wignall and Twitchett, 1996), the increase of atmospheric CO_2 content (Berner, 2002), global warming (Huey and Ward, 2005), carbon isotopic excursion (Payne et al., 2004), acid rain, etc. (Liang, 2002; Maruoka et al., 2003).

The reason of the most severe mass extinction in the geologic record is a hot research subject in the earth science. One of the hypotheses is that the mass extinction event is usually caused by extraterrestrial body impact, as evidenced by Ir anomalies found at the K/T boundary. But there is a controversy at the evidence of extraterrestrial body impact in the P-T boundary event. Xu et al. (1985) analyzed the clay layer samples from the Meishan P/Tr boundary section, China. The results showed that the content of Ir is about 2 ng/g, which is obviously higher than the background values of the crust, and the Ir anomalies were not confirmed in later studies (Clark et al., 1986; Zhou and Kyte, 1988; Cai et al., 1986). As reported by Becker et al. (2001), the extraterrestrial noble gas ^{3}He was found for the first time in the same P/Tr boundary section at Meishan, Changxing County, Zhejiang Province, China, which may imply an extraterrestrial source. Some similar research results were reported

from the P/Tr boundary section at Graphite Peak, Antarctica (Poreda and Becker, 2003). However, Farley et al. (2001) analyzed the samples collected from the Meishan section and found no extraterrestrial ^{3}He. Another evidence for a bolide impact is the discovery of chondritic fragments in the P-Tr boundary section in Antarctica (Basu et al., 2003), but this finding cannot be reproduced. Beside extraterrestrial bolide impact, more evidence shows that the mass extinction which happened in the P/Tr boundary period is genetically caused by vast flood volcanism that caused catatrophic changes of the ecosystem (Courtillot et al., 1999; Wignall, 2001; Grard et al., 2005). The P/Tr boundary event occurred about 252.28±0.08 Ma years ago (Shen et al., 2011), which is almost the same period during which Siberian basalt eruption took place (Renne et al., 1995; Reichow et al., 2002; Kamo et al., 2003; Mundil et al., 2004). In addition, the time of Emeishan basalt eruption in Sichuan Province, China, partly overlaps with that in the P/Tr boundary section (Boven et al., 2002; Lo et al., 2002), or earlier than the latter (Guo et al., 2004; Zhou et al., 2006; He et al., 2007).

Zhou and Kyte (1988) analyzed the clay layer samples from the P/Tr boundary section in Meishan and other areas in China. The results showed that Cs, Zr, Hf, Ta and Th were strongly enriched while Cr, Co and Ir were strongly depleted, suggesting that the source of clay is related with volcanic ash. Xu et al. (2007) analyzed systematically the contents of PGEs, including Ir, from the Meishan P/Tr boundary section. The result showed that there is no Ir anomaly, and the patterns of PGEs in the P/Tr boundary section at Meishan are similar with those of Siberial and Emeishan basalts, which are different from the known extraterrestrial materials. This result further indicated the correlation between the mass extinction event in the P/Ts boundary period and the large-scale volcanic activity. Analyzing the samples from the Meishan section, Shen et al. (2011) also found evidence of fire burning and volcanic activity leading to anoxia, which led to changes in the environment (Shen and Lin, 2010; Shen et al., 2007).

In order to find out the evidence of mass extinction event at the P/Tr boundary, the late Jin Yugan (an academician) working at the Nanjing Institute of Geology and Palaeontology and Prof. Kyte F. coming from the California Institute of Technology, USA, organized the International Cooperation Project of "Chinese Meishan Permian-Triassic (P/T) Extinction Event" to carry out a comprehensive study in many aspects, including paleontology, petrography and mineralogy, magnetic stratigraphy, isotopes (such as O, C, S, Sr, etc.), element geochemistry (such as REE, PGEs), organic geochemistry (such as organic carbon, biomarker, etc.), fullerene, rare gas, etc., with an attempt to analyze the two drilling samples from the Global Stratotype Section and Point (GSSP) of the P/Tr boundary at Meishan, Changxing County, Zhejiang Province, China, in combination with the famous global geochemical laboratories. The project is expected to get a clear conclusion that whether the mass extinction at the P/Tr boundary section is related to the extraterrestrial bolide impact event. In this study, we will report the research results concerned.

2 Samples and experiment

The Meishan section in Changxing County, Zhejiang Province, China, is the global stratotype section and point (GSSP) of the P/Tr boundary, also known as "golden spike" (Yin, 2001). The section located at a series of large quarries, which is divided into A, B, C, D, E and Z in turn from west to east. The samples used in the study were collected from Bed 24 to Bed 28 (Yin et al., 1996; Zhao et al., 1981; Sheng et al., 1987). Among them, Bed 24 is mainly composed of limestone, at the top of which is pyrite lamina. Bed 25 is composed of white clay, and Bed 26 is composed of black clay. Bed 27 is divided into four layers a, b, c and d from the top to the bottom, which are mainly composed of limestone. Bed 28 is composed of white clay. The boundary between the layers of Bed 27b and 27c at Quarry D was defined as the GSSP of the P/Tr boundary according to the first appearance of *Hindeodusparvus* (Yin et al., 1996, 2001, 2005), which belong to the biological boundary layer. However, the P/T catastrophec event (or geochemical) boundary lies about 10 cm below, recognized as the "boundary clay" of Beds 25 and 26 or probably the pyrite lamina on the top of Bed 24e (Bowring et al., 1998; Jin et al., 2000; Yin et al., 2001, 2005).

In order to ensure the samples to be as fresh as possible and to avoid contamination, the drill core samples were used in the study. The drilling sites were located 550 m (Meishan-1) and 150 m (Meishan-2) west of section D of the Meishan P/Tr boundary. By drilling through the P/Tr boundary layer, the core samples are very intact and fresh (2003). All the samples were of unified treatment for crushing, grinding and distribution at the sedimentology laboratory of the National History Museum. In order to verify the results obtained by different laboratories, the samples were numbered randomly, which were distributed to different laboratories in the form of unknown samples. The number for the actual section of samples will be told to the researchers from different laboratories after all laboratories have completed their analyses of the samples and submitting the analytical results. Figure 1 shows the actual position of numbered samples from the Meishan section.

The VG Plasma-Quad ExCell ICP-MS installed

at the National Research Center for Geological Analysis has been employed in this study (Chinese Academy of Geological Sciences). The multi-element solution of 20×10^{-9} produced by U.S.A. was used. All samples were separated and concentrated before determination.

The analytical method is isotope dilution and inductively coupled plasma mass spectrometry (ID-ICP-MS) combined with Te-coprecipitation that follows the improved method described by Qi et al. (2004). About 12 ng Pt, 10 ng Pd, 0.4 ng Ir and 0.7 ng Ru enriched isotope spikes were added in each sample. Silicates in the samples were dissolved with 45 mL of concentrated HF that was added in two times. 15 mL of *aqua regia* were added in the residue and heated to 80℃ for 1 hour, and then slowly evaporated to dryness. The treatment with *aqua regia* was repeated once. Any remained HNO_3 was then driven out by adding 8 mL of concentrated HCl, and evaporated to dryness. Finally, the dried fraction was dissolved in 15 mL of concentrated HCl and 10 mL of water, and transferred into a 50 mL centrifuge tube. After centrifugation, the solution was transferred into a 200 mL Savillex beaker. 35 mL of 3% H_3BO_3 was added in the residue to dissolve fluorides, followed by centrifugation. The process of dissolving fluorides with H_3BO_3 was repeated 3–5 times until the residue was <0.1 g. The last residue was fused with Na_2O_2 (<0.4 g), and then dissolved with water and HCl. This solution was added into the Savillex beaker.

The PGEs in the solutions were separated from the matrix through Te-coprecipitation by adding 2 mL of 1 mg/mL Te and 4 mL of 1 M $SnCl_2$. The solutions were then filtered using a millipore membrane filter (type-HA, 0.45 μm). The Te precipitants were dissolved in 2 mL of *aqua regia*, and diluted to 10 mL for passing through the ion exchange column (glass columns with a reservoir at the top, 5 mm×120 mm) to eliminate interferences of Cu, Ni, Zr and Hf. The column consists of cation exchange resin of Dowex 50 WX8 (200–400 mesh, 2 g) and P507 extraction chromatograph resin (60–80 mesh, 1 g). The elution solutions were diluted to 5 mL for ICP-MS measurement, and the acidity is within the range of 3%–4%.

All of the HF, HCl and HNO_3 used in this study were sub-boiling purified. High-purity deionized water (18 MΩ/cm) was obtained from a Milli-Q system. The $SnCl_2$ and Te solutions were purified by Te-coprecipitation with each other. The H_3BO_3 solution was also purified by Te-coprecipitation. The blank level and determination limit of the ID-ICP-MS method are given in Table 1. The blank level is the average of six analyses of blanks that were prepared in the same way as the samples, i.e., Ir 0.0002 ng/g, Ru 0.0019 ng/g, Rh 0.0002 ng/g, Pt 0.0106 ng/g and Pd 0.0016 ng/g. The determination limit is taken as 10 times the standard deviation of the counts of the blanks divided by the sensitivity 10 ng/mL PGE standard solutions, i.e., Ir 0.0029 ng/g, Ru 0.0057 ng/g, Rh 0.0011 ng/g, Pt 0.0289 ng/g and Pd 0.0222 ng/g. The abundances of Ir, Ru, Pt and Pd were calculated by the isotope dilution method. Rh is a mono-isotope, hence it was calculated using ^{194}Pt as the internal standard.

The results of analysis of reference material WGB-1 are listed in Table 1. Although lower than the certified values, our results are consistent with other literature data analyzed with ID-ICP-MS and NiS. The discrepancy of Rh is probably attributable to the analytical methods. Except that the abundances of Ir and Pt are lower, our data are consistent with what was reported by Qi et al. (2004), which is higher than what was reported by Meisel et al. (2001), and Jin and Zhu (2000).

3 Results

We analyzed a total of 16 pieces of samples selected from three sections, including Section B with 9 pieces of samples from Bed A to Bed H and Bed T, Section C only with Bed N, and Section C with 6 pieces of samples from Bed O to Bed S and Bed U. Our data on the P/Tr boundary samples revealed no obvious positive Ir anomaly, with a range of 0.003–0.029 ng/g (Table 1). Variations in the concentrations of Ir and other PGEs between Sections B and C are shown in Fig. 1. The abundances of Ir and other PGEs reach the maximum at Bed 26, and Bed 25 and the pyrite lamina of Bed 24 (Bed C and Bed Q) contains the lowest abundance of those PGEs. Bed 25 and pyrite lamina of Bed 24 are generally referred to as the P/Tr event boundary, but they contain very low Ir. On the contrary, the abundances of Ir and other PGEs in Bed 27 and at the top of Bed 24 are higher than those of Bed 25 and pyrite lamina of Bed 24. Bed G is enriched in carbon and overlaps the top of Bed F. With the exception of Ru, the contents of the other PGES in Bed G are obviously higher than those of Bed F. The abundances of PGEs are different from one layer to another, but they have the same pattern. The concentrations of PGEs in Sections B and C have the same results, which have testified that our data are more reliable.

Figure 1 shows the Ir and Pd concentration profiles of the Meishan P/Tr boundary section are parallel. Plotted in Fig. 2 are the CI-normalized abundances of PGEs of the samples, indicative of the highly fractionated patterns with the relative abundance increasing from left to right (in the order of volatility). The PGE patterns of individual samples are nearly parallel to each other, except for slightly higher Ru at Bed F from Section B and Bed Q from Section C, and Rh at Bed N from Section C.

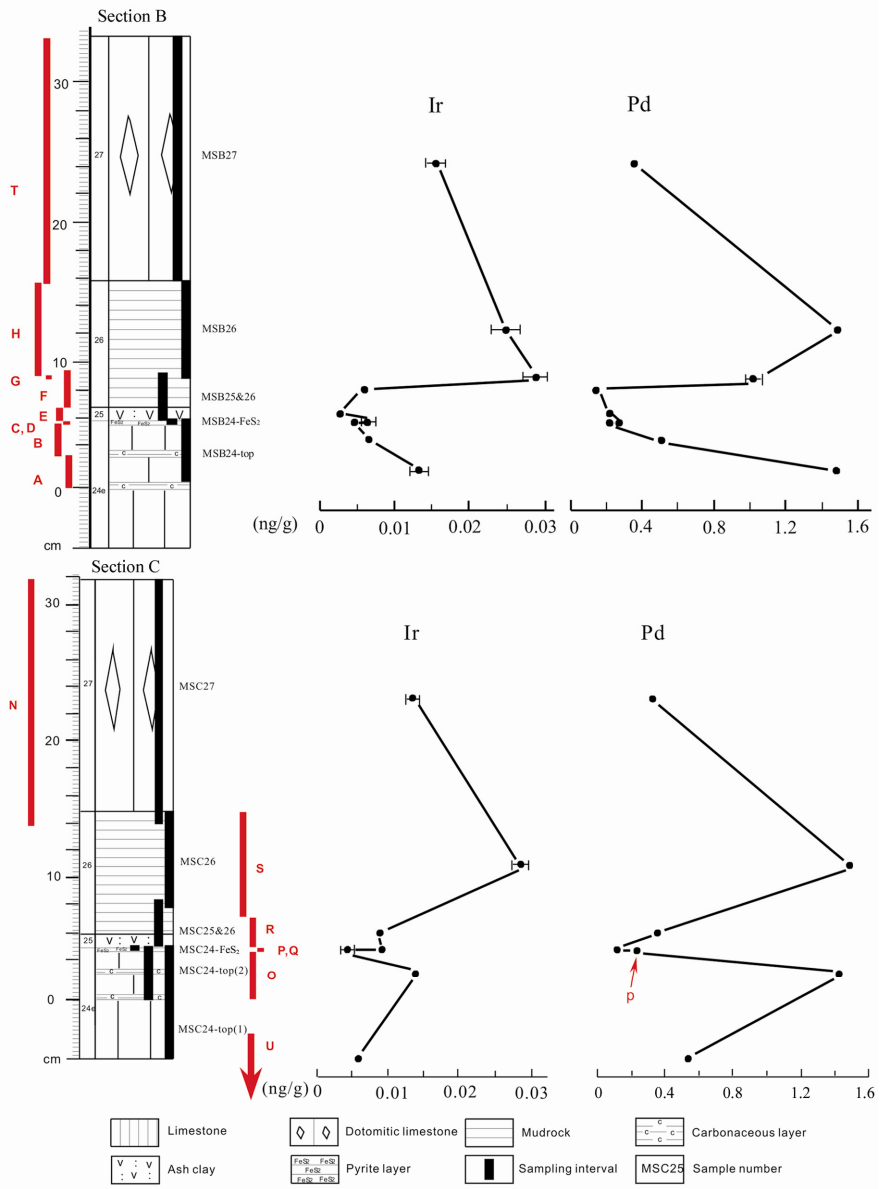

Fig. 1. Ir and Pd concentration profile of the Meishan P/Tr boundary section. Ir and Pd concentration profiles at Sections B and C of the Meishan P/Tr boundary section, showing small peaks at Bed 26. The abundances of Ir and Pd in Bed 27 and at the top of Bed 24e are higher than those of Bed 25 and pyrite lamina of Bed 24 that were the P/Tr event boundary in all probability. The sample numbers in this study correspond to the actual section of samples (marked by red).

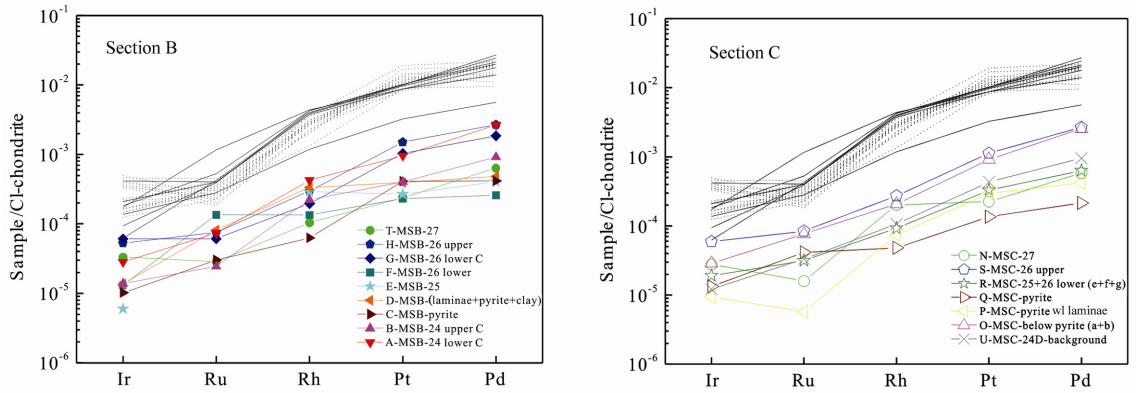

Fig. 2. PGE patterns of samples from the Meishan P/Tr boundary section.

Table 1 PGEs concentrations of the Meishan P/Tr boundary section (ng/g)

	Layer	Ir			Ru			Rh			Pt			Pd			Note
MSB-24e lower C	A	0.014	±	0.001	0.053	±	0.004	0.057	±	0.001	0.952	±	0.011	1.493	±	0.009	This study
MSB24e upper C	B	0.007	±	0.0003	0.017	±	0.004	0.030	±	0.0004	0.398	±	0.001	0.513	±	0.008	This study
MSB-pyrite	C	0.005	±	0.0002	0.021	±	0.005	0.008	±	0.0005	0.407	±	0.006	0.233	±	0.002	This study
MSB-laminae+ pyrite+clay	D	0.007	±	0.001	0.058	±	0.002	0.045	±	0.0004	0.389	±	0.001	0.271	±	0.006	This study
MSB-25	E	0.003			n.d.			0.039			0.265			0.226			This study
MSB-26 lower	F	0.006	±	0.0003	0.097	±	0.002	0.018	±	0.0003	0.228	±	0.009	0.145	±	0.008	This study
MSB-26 lower including C	G	0.029	±	0.002	0.044	±	0.012	0.026	±	0.002	1.020	±	0.015	1.040	±	0.046	This study
MSB-26 upper	H	0.025	±	0.002	0.054	±	0.006	0.040	±	0.001	1.500	±	0.005	1.500	±	0.008	This study
MSB-27	T	0.016	±	0.001	0.020	±	0.004	0.014	±	0.001	0.236	±	0.010	0.356	±	0.007	This study
MSC-27	N	0.013	±	0.001	0.011	±	0.003	0.027	±	0.001	0.222	±	0.007	0.323	±	0.003	This study
MSC-below pyrite (a+b)	O	0.014	±	0.0002	0.054	±	0.006	0.028	±	0.0004	0.907	±	0.002	1.430	±	0.018	This study
MSC-pyrite+laminae	P	0.005	±	0.001	0.004	±	0.009	0.010	±	0.0005	0.293	±	0.003	0.234	±	0.005	This study
MSC-pyrite	Q	0.006	±	0.002	0.030	±	0.012	0.006	±	0.0003	0.134	±	0.003	0.120	±	0.009	This study
MSC-25+26 lower (e+f+g)	R	0.009	±	0.0003	0.022	±	0.002	0.012	±	0.001	0.326	±	0.009	0.354	±	0.010	This study
MSC-26 upper	S	0.028	±	0.001	0.060	±	0.008	0.037	±	0.0000	1.120	±	0.004	1.500	±	0.008	This study
MSC-24D-background	U	0.006	±	0.0002	0.024	±	0.005	0.014	±	0.0004	0.428	±	0.004	0.534	±	0.005	This study
Blank		0.0002			0.002			0.0002			0.011			0.002			This study
Determination limits		0.003			0.006			0.001			0.029			0.022			This study
Reference material WGB-1		0.141	±	0.025	0.116	±	0.014	0.198	±	0.006	4.339	±	0.788	10.67	±	0.431	This study
		0.153	*±*	*0.026*	*0.144*	*±*	*0.079*	*0.167*	*±*	*0.011*	*5.25*	*±*	*0.95*	*11.5*	*±*	*1.4*	*Xu et al., 2007*
		0.204	*±*		*0.215*			*0.326*			*5.04*			*12.6*			*Xu et al., 2007*
		0.33			*0.30*			*0.32*			*6.10*			*13.9*			*recommended*
		0.23	*±*	*0.02*	*0.16*	*±*	*0.04*	*0.19*	*±*	*0.02*	*5.74*	*±*	*0.65*	*12.0*	*±*	*1.7*	*Qi et al., 2004*
		0.27			*0.16*						*4.71*			*11.7*			*Meisel*
		0.20	*±*	*0.04*	*0.20*	*±*	*0.04*	*0.14*	*±*	*0.01*	*3.8*	*±*	*1.0*	*13.0*	*±*	*1.1*	*Plessen, 1998*
		0.20	*±*	*0.02*	*0.17*	*±*	*0.03*	*0.15*	*±*	*0.01*	*4.20*	*±*	*0.50*	*12.90*	*±*	*0.5*	*Jin et al., 2000*

Note: Blank refers to the average value of 3 blank samples; Determination limits are 10 times the standard deviation of 3 blank samples. n.d.=below the determination limit. The results are given as mean±σ. Literature data (italic) after Xu et al. (2007); Qi et al. (2004); Meisel et al. (2001); Plessen and Erzinger (1998); and Jin and Zhu (2000).

The CI-normalized PGE patterns of the Meishan P/Tr boundary section are highly fractionated, the abscissa indicates the increase of relative abundances of the elements from left to right according to 50% condensation temperature. The patterns of all the samples we analyzed are nearly parallel to each other, followed along with an increase in melt degree of PGEs, the patterns are more mildly. The Siberian basalts (solid lines) (Lightfoot and Keays, 2005) and Emeishan basalts (dotted lines) (Song et al., 2006) are shown for comparison, which are also parallel to the Meishan P/Tr boundary samples, especially the Siberian basalts have a good coherence, and Emeishan basalts have slightly higher Pt and depleted Ru.

4 Discussion

The Ir anomaly is one piece of the crucial evidence for extraterrestrial impacts responsible for mass extinction in the P/Tr event boundary sections (Xu et al., 1985). Xu et al. (1985) analyzed Ir of the Meishan P/Tr boundary section using RNAA, and reported an Ir concentration of 2 ng/g. Our data showed that the Ir concentrations both in Sections B and C of the Meishan section are lower than those reported by Xu et al. (1985) but are consistent with those (0.003–0.087 ng/g) reported by Zhou and Kyte (1988) for the same section.

This discrepancy of Ir anomaly could not be attributed to the heterogeneous distribution of PGEs in the samples. Our several groups of data on PGEs of the Meishan boundary section are very consistent each other (Xu et al., 2007). In comparison with small pieces (80–120 mg) of samples for RNAA, much larger samples (about 100 mg) were used in our analysis, hence the results are more representative.

Pyrite laminae at the top of Bed 24e (Beds C and Q) are like those at the P/Tr event boundary, in which there has been a sharp change in ^{13}C (Jin et al., 2000), ^{34}S and ^{87}Sr (Kaiho et al., 2001). And the captured ^{3}He-enriched noble gases were also reported in samples at the base of Bed 25 of the Meishan section (Becker et al., 2001). But our data show that the pyrite laminae at the top of Bed 24e and Bed 25 have the lowest concentrations of Ir and the other PGEs. Xu et al. (2007) analyzed the samples from Bed 28 overlying Bed 27, and the results showed that Ir and the other PGEs are obviously higher than those in the mass extinction event section. According to the variation patterns at different layers, there has no PGEs anomaly. In addition, no solid shocked minerals including Fe-Ni grains were observed in the event beds.

The more important evidence is that the highly fractionated patterns of PGEs in the Meishan P/Tr boundary section are different from those of chondrites (Fig. 3). Although some iron meteorites have experienced high fractionation of PGEs, the patterns are different (Fig. 4). It is clearly seen that the PGEs of the Meishan P/Tr boundary section do not come from chondritic or iron meteorites. Most of the meteorites (>98% in number) are chondrites and iron meteorites, so we can rule out the possibility that the mass extinction event of the Meishan boundary section is due to extraterrestrial impacts.

In addition, Figure 2 shows very similar PGEs patterns between the Meishan samples we analyzed and the Siberian flood basalts and Emeishan flood basalts, particularly closely parallel to the former. The above-mentioned relations indicated that the PGEs of the Meishan P/Tr boundary section were derived from the Siberian flood basalts and(or) Emeishan blood basalts.

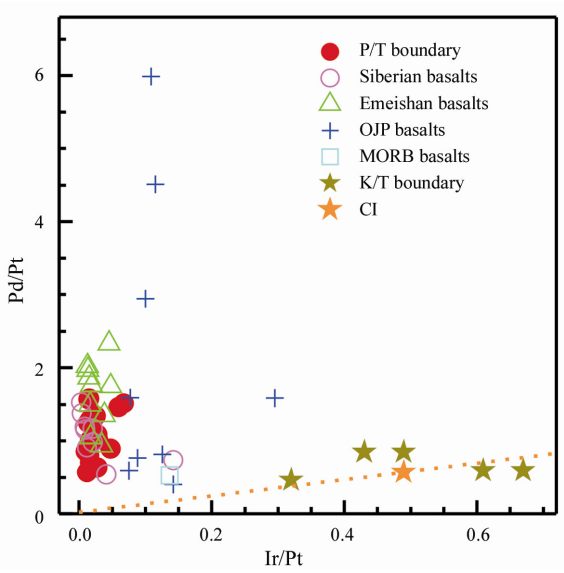

Fig. 3. Ir/Pt vs. Pd/Pt plots of the Meishan P/Tr boundary section. Note: (a) Our analyses of the Meishan samples are evidently different from literature values for the K/T boundary section (Kyte et al., 1985; Lee et al., 2003), which are overlapped with those of CI chondrites. A dashed line shows the chondritic ratio of Pd/Ir as a reference. (b) The inset shows similarity of the Meishan samples with the Siberian basalts (Lightfoot and Keays, 2005) and Emeishan basalts (Song et al., 2006), except for a higher Ir/Pt ratio of the Gd unit that is located at the bottom of the Siberian trap. In contrast, the mid-ocean ridge basalts (MORB) and the Ontong Java Plateau (OJP) basalts (Ely and Neal, 2003) have distinguishable ratios. Data of the CI chondrites are from Anders and Grevesse (1989).

Plotted in Fig. 3 are element ratios with Ir/Pt vs. Pd/Pt. It is clear that the Meishan boundary samples are consistent with the Siberian flood basalts and Emeishan flood basalts, and are far from the chondritic meteorites and other basalts. Compared with samples from the K/T boundary section, the mass ex-

tinction event is due to extraterrestrial impacts and this viewpoint has been commonly accepted, the PGE ratios fall within the range of those of chondritic meteorites.

The zircon U-Pb ages of the Siberian flood basalts are within the range of 249.4–250 Ma (Renne et al., 1995; Reichow et al., 2002; Kamo et al., 2003). Although there has been reported that many zircon U-Pb ages of the Emeishan flood basalts are similar to those of the Siberian flood basalts (Lo et al., 2002), most studies showed that there are much older ages (Zhou et al., 2006; He et al., 2007). The zircon U-Pb ages of the P/Tr boundary ashes are within the range of 250.0–251.4 Ma (Renne et al., 1995; Bowring et al., 1998), which are in synchrony with eruption of the Siberian flood basalts. So the PGEs are more possibly derived from the Siberian flood basalts.

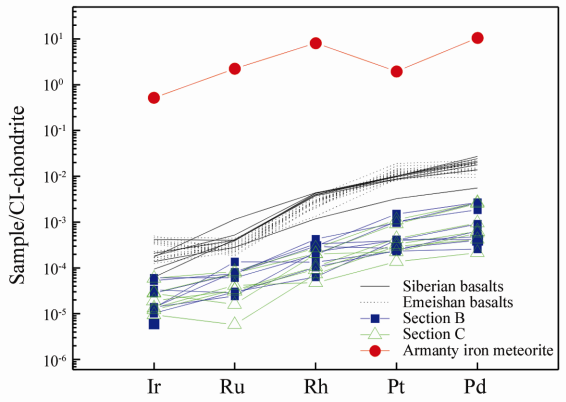

Fig. 4. The partial area of PGEs patterns from the Armanty iron meteorite. Figure 4 shows an area (labeled it as L1 in literature) of the PGEs patterns from the Armanty (IIIE) iron meteorite has experienced high fractionation of PGEs (Xu et al., 2008), but the patterns are different from those of the Meishan P/Tr boundary section and Siberian basalts and Emeishan basalts.

Dark-colored clay in Bed 26 may be indicative of the existence of organic matter, a comparison of the C-bearing Bed G in Section B with samples from Bed F (the bottom of Bed 26) demonstrated that carbon made a certain contribution to the increase of PGE content. But the maximum values of the PGEs, except for Ir, are reported from Bed H above Bed 26 (overlying the C-bearing Bed G). Such a significant difference could hardly be the result of bio-processes because Bed 26 and the pyrite bed as well other rock beds all have similar PGE distribution patterns.

The PGEs patterns of the Meishan P/Tr boundary section are similar to those of Bed 24e to Bed 28 (Xu et al., 2007), suggestive of their similar sources. And their wide time range at layers is consistent with the long-term eruption of the Siberian flood basalts, different from the short-time extraterrestrial impacts.

Assuming all PGEs were contributed by the Siberian basalts, the contents of basaltic ashes in individual beds can be estimated according to their PGE abundances. The results showed that the maximum content of the basaltic ashes was found in Bed 26, only accounting for about 20%. This implies that the clay of Bed 25 and Bed 26 is composed of other highly PGE-depleted volcanic ashes.

A large volume of fine framboid pyrite, at the same time, similar to what had been observed previously, occurred in the event bed, indicative of anoxic to dysoxic depositional environments in the Meishan section (Shen et al., 2007). It is particularly noteworthy that a great proportion of bioclastic pyrite as well as fine framboid pyrite grains is preserved in the pyrite crust which lies on the top of Bed 24e. The fact that the sulfur isotope of pyrite crust approaches to 0‰ (Liang and Ding, 2004; Jiang et al., 2006) is consistent with intensive volcanic activities. The co-occurrence and causal links of mass extinction, anoxia and intensive volcanic activities in the event bed suggest that volcanism would be most likely to be the ultimate reason for environmental change and biomass crisis. Large quantities of hazardous gases emitted into air and volcanic sulfur (including H_2S) entered oceanic water, resulting in hypoxia and poisoning of ocean water and anoxia, thus leading to simultaneous extinction of both continental and oceanic biomass.

Acknowledgements This research project was financially supported by the National Natural Science Foundation of China (No. 41073053).

References

Anders E. and Grevesse N. (1989) Abundances of the elements: Meteoritic and solar [J]. *Geochimica et Cosmochimica Acta.* **53**, 197–214.

Basu A.R., Petaev M.I., Poreda R.J., Jacobsen S.B., and Becker L. (2003) Chondritic meteorite fragments associated with the Permian-Triassic boundary in Antarctica [J]. *Science*. **302**, 1388–1392.

Becker L., Poreda R.J., Hunt A.G., Bunch T.E., and Rampino M. (2001) Impact event at the Permian-Triassic boundary: Evidence from extraterrestrial noble gases in fullerenes [J]. *Science.* **291**, 1530–1533.

Benton M.J., Tverdokhlebov V.P., and Surkov M.V. (2004) Ecosystem remodelling among vertebrates at the Permian-Triassic boundary in Russian [J]. *Nature*. **432**, 97–100.

Berner R.A. (2002) Examination of hypotheses for the Permo-Triassic boundary extinction by carbon cycle modeling [J]. *Proceedings of the National Academy of Sciences of the United States of America.* **99**, 4172–4177.

Bowring S.A., Erwin D.H., Jin Yugan, Martin M.W., Davidek K., and Wang Wei (1998) U/Pb zircon geochronology and tempo of the End-Permian mass extinction [J]. *Science.* **280**, 1039–1045.

Clark D.L., Wang C., Orth C.J., and Gilmore J.S. (1986) Conodont survival and low iridium abundance across the Permian-Triassic boundary in

South China [J]. *Science*. **233**, 984–986.

Courtillot V., Jaupart C., Manighetti I., Tapponnier P., and Besse J. (1999) On causal links between flood basalts and continental breakup [J]. *Earth and Planetary Science Letters*. **166**, 177–195.

Ely J.C. and Neal C.R. (2003) Using platinum-group elements to investigate the origin of the Ontong Java Plateau, SW Pacific [J]. *Chemical Geology.* **196** (1–4). 235–257.

Erwin D.H. (1994) The Permo-Triassic extinction [J]. *Nature*. **367**, 231–236.

Farley K.A., Mukhopadhyay, Isozaki Y., Becker L., and Poreda R.J. (2001) An extraterrestrial impact at the Permian-Triassic Boundary? [J]. *Science*. **293**, 2343a.

Grard A., Francois L.M., Dessert C., Dupre B., and Godderis Y. (2005) Basaltic volcanism and mass extinction at the Permo-Triassic boundary: Environmental impact and modeling of the global carbon cycle [J]. *Earth and Planetary Science Letters*. **234**, 207–221.

He Bin, Xu Yigang, Huang Xiaolong, Luo Zhenyu, Shi Yuruo, Yang Qijun, and Yu Songyue (2007) Age and duration of the Emeishan flood volcanism, SW China: Geochemistry and SHRIMP zircon U-Pb dating of silicic ignimbrites, post-volcanic Xuanwei Formation and clay tuff at the Chaotian section [J]. *Earth and Planetary Science Letters.* **255**(3–4), 306–323.

Huey R.B. and Ward P.D. (2005) Hypoxia, global warming, and terrestrial Late Permian extinctions [J]. *Science*. **308**, 398–401.

Jiang Yaofa, Tang Yuegang, Dai Shifeng, Zou Xing, Qian Handong, and Zhou Guoqing (2006) Pyrites and sulfur isotopic composition near the Permian-Triassic boundary in Meishan, Zhejiang [J]. *Acta Geological Sinica.* **80**, 1202–1207.

Jin Xindi and Zhu Heping (2000) Determination of platinum group elements and gold in geological samples with ICP-MS using a sodium peroxide fusion and tellurium co-precipitation [J]. *Journal of Analytical Atomic Spectrometry.* **15**, 747–751.

Jin Yugan, Wang Yue, Wang Wei, Shang Qinghua, Cao Changqun, and Erwin D.H. (2000) Pattern of marine mass extinction near the Permian-Triassic Boundary in South China [J]. *Science.* **289**, 432–436.

Kaiho K., Kajiwara Y., Nakano T., Miura Y., Kawahata H., Tazaki K., Ueshima M., Chen Z., and Shi G.R. (2001) End-Permian catastrophe by a bolide impact: Evidence of a gigantic release of sulfur from the mantle [J]. *Geology.* **29**, 815–818.

Kamo S.L., Czamanske G.K., Amelin Y., Fedorenko V.A., Davis D.W., and Trofimov V.R. (2003) Rapid eruption of Siberian flood-volcanic rocks and evidence for coincidence with the Permian-Triassic boundary and mass extinction at 251 Ma [J]. *Earth and Planetary Science Letters.* **214**(1–2), 75–91.

Kyte F.T., Smit J., and Wasson J.T. (1985) Siderophile interelement variations in the Cretaceous-Tertiary boundary sediments from Caravaca, Spain [J]. *Earth Planetary Science Letters.* **73**, 183–195.

Lee C.-T.A., Wasserburg G.J., and Kyte F.T. (2003) Platinum-group elements (PGE) and rhenium in marine sediments across the Cretaceous-Tertiary boundary: Constraints on Re-PGE transport in the marine environment [J]. *Geochimica et Cosmochimica Acta.* **67**, 655–670.

Liang Handong and Ding Tiping (2004) Evidence of extremely light gypsum from the Permian-Triassic (P/T) event boundary at the Meishan section of South China [J]. *Acta Geoscientica Sinica.* **25**, 33–37.

Liang Handong (2002) End-Permian catastrophic event of marine acidification by hydrated sulfuric acid: Mineralogical evidence from Meishan Section of South China [J]. *Chinese Science Bulletin*. **47**, 1393–1397.

Lightfoot P.C. and Keays R.R. (2005) Siderophile and chalcophile metal variations in flood basalts from the Siberian trap, Noril'sk region: Implications for the origin of the Ni-Cu-PGE sulfide ores [J]. *Economic Geology.* **100**, 439–462.

Lo Chinghua, Chung Sunlin, Lee Tungyi, and Wu Genyao (2002) Age of the Emeishan flood magmatism and relations to Permian-Triassic boundary events [J]. *Earth and Planetary Science Letters.* **198**, 449–458.

Maruoka T., Koeberl C., Hancox P.J., and Reimold W.U. (2003) Sulfur geochemistry across a terrestrial Permian-Triassic boundary section in the Karoo Basin, South Africa [J]. *Earth and Planetary Science Letters*. **206**(1–2), 101–117.

Meisel T., Moser J., Fellner N., Wegscheider W., and Schoenberg R. (2001) Simplified method for the determination of Ru, Pd, Re, Os, Ir and Pt in chromitites and other geological materials by isotope dilution ICP-MS and acid digestion [J]. *Analyst.* **126**, 322–328.

Mundil R., Ludwig K.R., Metcalfe I., and Renne P.R. (2004) Age and timing of the Permian mass extinction: U/Pb dating of closed-system zircons [J]. *Science*. **305**, 1760–1763.

Payne J.L., Lehrmann D.J., Wei J., Orchard M.J., Schrag D.P., and Knoll A.H. (2004) Large perturbations of the carbon cycle during recovery from the End-Permian extinction [J]. *Science*. **305**, 506–509.

Plessen H.G. and Erzinger J. (1998) Determination of the platinum-group elements and gold in twenty rock reference materials by inductively coupled plasma-mass spectrometry (ICP-MS) after pre-concentration by nickel sulfide fire assay [J]. *Geostandards Newsletter*. **22**, 187–194.

Poreda R.J. and Becker L. (2003) Fullerene and interplanery dust at the Permian-Triassic Boundry [J]. *Astrobiology*. **3**, 75–90.

Qi Liang, Zhou Meifu, and Wang C.Y. (2004) Determination of low concentrations of platinum group elements in geological samples by ID-ICP-MS [J]. *Journal of Analytical Atomic Spectrometry.* **19**, 1335–1339.

Reichow M.K., Saunders A.D., White R.V., Pringle M.S., Al'Mukhamedov A.I., Medvedev A.I., and Kirda N.P. (2002) $^{40}Ar/^{39}Ar$ dates from the West Siberian Basin: Siberian Flood Basalt Province Doubled [J]. *Science*. **296**, 1846–1849.

Renne P.R., Black M.T., Zhang Z., Richards M.A., and Basu A.R. (1995) Synchrony and causal relations between Permian-Triassic boundary crises and Siberian flood volcanism [J]. *Science*. **269**, 1413–1416.

Shen Wenjie and Lin Yangting (2010) Environmental conditions and events prior to the Permian-Triassic boundary at Meishan section, China [J]. *Journal of Earth Science*. **21**(special), 151–153.

Shen Wenjie, Lin Yangting, Xu Lin, Li Jianfeng, Wu Yasheng, and Sun Yongge (2007) Pyrite framboids in the Permian–Triassic boundary section at Meishan, China: Evidence for dysoxic deposition [J]. *Palaeogeography, Palaeoclimatology, Palaeoecology*. **253**, 323–331.

Shen Wenjie, Sun Yongge, Lin Yangting, Liu Dehan, and Chai Pingxia (2011) Evidence for wildfire in the Meishan section and implications for Permian-Triassic events [J]. *Geochimica et Cosmochimica Acta*. 75, 1992–2006.

Song Xieyan, Zhou Meifu, Keays R.R., Cao Zhimin, Sun Min, and Qi Liang (2006) Geochemistry of the Emeishan flood basalts at Yangliuping, Sichuan, SW China: Implications for sulfide segregation [J]. *Contributions to Mineralogy and Petrology*. **152**, 53–74.

Wignall P.B. (2001) Large igneous provinces and mass extinctions [J]. *Earth Science Reviews*. **53**(1–2), 1–33.

Wignall P.B. and Twitchett R.J. (1996) Oceanic anoxia and the Permian mass extinction [J]. *Science*. **272**, 1155–1158.

Xu Daoyi, Ma Shulan, Chai Zhifang, Mao Xueying, Sun Yiying, Zhang Qinwen, and Yang Zhengzhong (1985) Abundance variation of iridium and trace elements at the Permian/Triassic boundary at Shangsi in China [J]. *Nature*. **314**, 154–156.

Xu Lin, Ling Yangting, Shen Wenjie, Qi Liang, Xie Liewen, and Ouyang Ziyuan (2007) Platinum-group elements of the Meishan Permian-Triassic boundary section: Evidence for flood basaltic volcanism [J]. *Chemical Geology*. **246**, 55–64.

Xu Lin, Miao B., Lin Yangting, and Ouyang Ziyuan (2008) Ulasitai: A new iron meteorite likely pairing with Armanty (IIIE) [J]. *MAPS*(in press).

Yin Hongfu, Tong Jinan, and Zhang Kexin (2005) A review on the global stratotype section and point of the Permian-Triassic boundary [J]. *Acta Geological Sinica*. **79**, 715–728.

Yin Hongfu, Zhang Kexin, Tong Jinan, Yang Zunyi, and Wu Shunbao (2001) The global stratotype section and point (GSSP) of the Permian-Triassic boundary [J]. *Episodes*. **24**, 102–114.

Yin Hongfu, Sweet W.C., Glenister B.F., Kotlyar G., Kozer H., Newell N.D., Sheng Jinzhang, Yang Zunyi, and Zakharov Y.D. (1996) Recommendation of the Meishan; section as Global Stratotype Section and Point for basal boundary of Triassic System [J]. *Newsletters on Stratigraphy*. **34**, 81–108.

Zhou Lei and Kyte F.T. (1988) The Permian-Triassic boundary event: Ageochemical study of three Chinese sections [J]. *Earth and Planetary Science Letters*. **90**, 411–421.

Zhou Meifu, Zhao Junhong, Qi Liang, Su Wenchao, and Hu Ruizhong (2006) Zircon U-Pb geochronology and elemental and Sr-Nd isotope geochemistry of Permian mafic rocks in the Funing area, SW China [J]. *Contributions to Mineralogy and Petrology.* **151**, 1–19.